

Measurement of the energy spectrum of underground muons at Gran Sasso with a transition radiation detector

The MACRO Collaboration

M. Ambrosio¹², R. Antolini⁷, C. Aramo^{7,n}, G. Auriemma^{14,a}, A. Baldini¹³, G. C. Barbarino¹², B. C. Barish⁴, G. Battistoni^{6,b}, R. Bellotti¹, C. Bemporad¹³, P. Bernardini¹⁰, H. Bilokon⁶, V. Bisi¹⁶, C. Bloise⁶, C. Bower⁸, S. Bussino¹⁴, F. Cafagna¹, M. Calicchio¹, D. Campana¹², M. Carboni⁶, M. Castellano¹, S. Cecchini^{2,c}, F. Cei^{11,13}, V. Chiarella⁶, B. C. Choudhary⁴, S. Coutu^{11,o}, L. De Benedictis¹, G. De Cataldo¹, H. Dekhissi^{2,17}, C. De Marzo¹, I. De Mitri⁹, J. Derkaoui^{2,17}, M. De Vincenzi^{14,e}, A. Di Credico⁷, O. Erriquez¹, C. Favuzzi¹, C. Forti⁶, P. Fusco¹, G. Giacomelli², G. Giannini^{13,f}, N. Giglietto¹, M. Giorgini², M. Grassi¹³, L. Gray^{4,7}, A. Grillo⁷, F. Guarino¹², P. Guarnaccia¹, C. Gustavino⁷, A. Habig³, K. Hanson¹¹, R. Heinz⁸, Y. Huang⁴, E. Iarocci^{6,g}, E. Katsavounidis⁴, E. Kearns³, H. Kim⁴, S. Kyriazopoulou⁴, E. Lamanna¹⁴, C. Lane⁵, D. S. Levin¹¹, P. Lipari¹⁴, N. P. Longley^{4,l}, M. J. Longo¹¹, F. Maaroufi^{2,17}, G. Mancarella¹⁰, G. Mandrioli², S. Manzoor^{2,m}, A. Margiotta Neri², A. Marini⁶, D. Martello¹⁰, A. Marzari-Chiesa¹⁶, M. N. Mazziotta^{1,*}, C. Mazzotta¹⁰, D. G. Michael⁴, S. Mikheyev^{4,7,h}, L. Miller⁸, P. Monacelli⁹, T. Montaruli¹, M. Monteno¹⁶, S. Mufson⁸, J. Musser⁸, D. Nicoló^{13,d}, C. Orth³, G. Osteria¹², M. Ouchrif^{2,17}, O. Palamara¹⁰, V. Patera^{6,g}, L. Patrizii², R. Pazzi¹³, C. W. Peck⁴, S. Petrera⁹, P. Pistilli^{14,e}, V. Popa^{2,i}, V. Pugliese¹⁴, A. Rainò¹, J. Reynoldson⁷, F. Ronga⁶, U. Rubizzo¹², C. Satriano^{14,a}, L. Satta^{6,g}, E. Scapparone⁷, K. Scholberg³, A. Sciubba^{6,g}, P. Serra-Lugaresi², M. Severi¹⁴, M. Sioli², M. Sitta¹⁶, P. Spinelli^{1,*}, M. Spinetti⁶, M. Spurio², R. Steinberg⁵, J. L. Stone³, L. R. Sulak³, A. Surdo¹⁰, G. Tarlè¹¹, V. Togo², D. Ugolotti², M. Vakili¹⁵, C. W. Walter³, and R. Webb¹⁵.

1. Dipartimento di Fisica dell'Università di Bari and INFN, 70126 Bari, Italy
2. Dipartimento di Fisica dell'Università di Bologna and INFN, 40126 Bologna, Italy
3. Physics Department, Boston University, Boston, MA 02215, USA
4. California Institute of Technology, Pasadena, CA 91125, USA
5. Department of Physics, Drexel University, Philadelphia, PA 19104, USA
6. Laboratori Nazionali di Frascati dell'INFN, 00044 Frascati (Roma), Italy
7. Laboratori Nazionali del Gran Sasso dell'INFN, 67010 Assergi (L'Aquila), Italy
8. Depts. of Physics and of Astronomy, Indiana University, Bloomington, IN 47405, USA
9. Dipartimento di Fisica dell'Università dell'Aquila and INFN, 67100 L'Aquila, Italy
10. Dipartimento di Fisica dell'Università di Lecce and INFN, 73100 Lecce, Italy
11. Department of Physics, University of Michigan, Ann Arbor, MI 48109, USA
12. Dipartimento di Fisica dell'Università di Napoli and INFN, 80125 Napoli, Italy
13. Dipartimento di Fisica dell'Università di Pisa and INFN, 56010 Pisa, Italy
14. Dipartimento di Fisica dell'Università di Roma "La Sapienza" and INFN, 00185 Roma, Italy
15. Physics Department, Texas A&M University, College Station, TX 77843, USA
16. Dipartimento di Fisica Sperimentale dell'Università di Torino and INFN, 10125 Torino, Italy
17. Also Faculty of Sciences, University Mohamed I, B.P. 424 Oujda, Morocco

- a* Also Università della Basilicata, 85100 Potenza, Italy
- b* Also INFN Milano, 20133 Milano, Italy
- c* Also Istituto TESRE/CNR, 40129 Bologna, Italy
- d* Also Scuola Normale Superiore di Pisa, 56010 Pisa, Italy
- e* Also Dipartimento di Fisica, Università di Roma Tre, Roma, Italy
- f* Also Università di Trieste and INFN, 34100 Trieste, Italy
- g* Also Dipartimento di Energetica, Università di Roma, 00185 Roma, Italy
- h* Also Institute for Nuclear Research, Russian Academy of Science, 117312 Moscow, Russia
- i* Also Institute for Space Sciences, 76900 Bucharest, Romania
- l* Swarthmore College, Swarthmore, PA 19081, USA
- m* RPD, PINSTECH, P.O. Nilore, Islamabad, Pakistan
- n* Also INFN Catania, 95129 Catania, Italy
- o* Also Department of Physics, Pennsylvania State University, University Park, PA 16801, USA

* Corresponding authors:

M.N.Mazziotta, e-mail: mazziotta@ba.infn.it

P.Spinelli, e-mail: spinelli@ba.infn.it

Abstract

We have measured directly the residual energy of cosmic ray muons crossing the MACRO detector at the Gran Sasso Laboratory. For this measurement we have used a transition radiation detector consisting of three identical modules, each of about 12 m^2 area, operating in the energy region from 100 GeV to 1 TeV. The results presented here were obtained with the first module collecting data for more than two years. The average single muon energy is found to be 320 ± 4 (stat.) ± 11 (syst.) GeV in the rock depth range 3000–6500 hg/cm². The results are in agreement with calculations of the energy loss of muons in the rock above the detector.

To be submitted to Astr. phys.

Introduction

High energy muons are produced in interactions of primary cosmic rays with nuclei in the Earth's atmosphere. The muon energy distribution is dependent on the spectrum and composition of the primary cosmic rays, and can be used to obtain information concerning these quantities. In particular, a direct measurement of the single muon spectra obtained deep underground can, in principle, provide information about the “all nucleon” cosmic ray spectra at high energies. This paper describes a measurement of the high energy underground muon spectrum, carried out using a transition radiation detector (TRD) in association with the MACRO detector.

An attempt was made in 1987 [1] to measure the residual energy of muons reaching the Mont Blanc underground laboratory. In this case, a small transition radiation detector (TRD) installed on the top of the NUSEX detector [2] provided the measurement of the muon energy in the range 100–500 GeV. The measured spectrum was consistent with a surface muon differential distribution of the type $E^{-3.71}$ folded with absorption in 5000 hg/cm² standard rock. More recently, a measurement of the cascade showers produced by underground muons inside the NUSEX calorimeter [3, 4] was used to obtain an average muon energy of $346 \pm 14 \pm 17$ GeV at a depth of 5000 hg/cm². The residual energy spectrum was reported to be “not in contradiction with a power law integral distribution with an index $\gamma=2.7-2.9$ ”.

To expand on these measurements, we have designed and built a large area TRD, for use in conjunction with the MACRO detector at the Gran Sasso Laboratory. The TRD allows the energy measurement of muons up to ~ 1 TeV, although with modest resolution. With this technique the energy of downgoing and of neutrino induced upgoing muons is measured directly. This allows the local spectrum and the average energy versus depth to be evaluated, independent of assumptions on the particle zenith angle distribution and of the energy losses in the surrounding rock [5].

1 The MACRO TRD

1.1 Properties of Transition Radiation

Transition radiation detectors are presently of interest for fast particle identification, both in accelerator experiments [6] and in cosmic ray physics [7-14]. In particular, TRDs have been proposed and developed to measure the energy of cosmic ray muons in the TeV region. The characteristic dependence of transition radiation on the Lorentz factor γ of the incident particle makes it possible to evaluate the energy $E = m_0\gamma c^2$ of the particle if the rest mass m_0 is known, as it is the case of atmospheric muons reaching an underground laboratory. TRDs can provide an energy measurement of particles over an energy range typically spanning one order of magnitude, between the transition radiation threshold and saturation energy values.

Transition radiation (TR) is emitted in the X-ray region whenever an ultrarelativistic charged particle crosses the boundary of two materials with different dielectric properties [16, 17]. At each interface the emission probability for an X-ray photon is of the order of $\alpha = 1/137$. Radiators consisting of several hundred regularly spaced foils are used to enhance X-rays production, allowing a reliable tagging of the fast particle.

The “multilayer” radiator introduces important physical constraints on the radiation yield, because of so-called “interference effects”. It has been established that the radiation emission threshold occurs at a Lorentz factor $\gamma_{th} = 2.5\omega_p d_1$, where ω_p is the plasma frequency (in eV

units) of the foil material, and d_1 is its thickness in μm [18]. At higher γ the radiation energy increases up to a saturation value given by $\gamma_{sat} \sim \gamma_{th}(d_2/d_1)^{1/2}$ [19], where d_2 is the width of the gap between the foils.

Similar behaviour has also been observed for irregular radiators such as carbon compound foam layers or fiber mats [7, 20], where the role of the thin foil is played by the cell wall and by the fiber element respectively, and the gap by the cell pore and by the fiber spacing. One important advantage of these materials is their low cost. In addition, their densities, and consequently the cell or fiber sizes and spacings, can be easily selected to produce increasing transition radiation in the Lorentz factor range $10^3 < \gamma < 10^4$, corresponding to a 100 GeV to 1 TeV energy region for muons. We have tested a variety of these materials, trying to obtain the maximum photon yield with minimum radiator thickness, while maintaining at the same time the widest range between γ_{th} and γ_{sat} [21].

Gaseous chambers working in the proportional region are generally preferred to solid state or scintillation counters for detection of transition radiation. In fact, the radiating particle, if not deflected by magnetic fields, releases its ionization energy in the same region as the X-ray photons, introducing a background signal that can be reduced if a gaseous detector is used. The gas must provide efficient conversion of the TR photons, leading to the use of high-Z gases such as argon, krypton, or xenon. Multiple module TRDs, with optimized gas layer thickness, are normally employed to improve the background rejection. A reduced chamber gap limits the particle ionizing energy losses, while those X-rays escaping detection may be converted in the downstream chambers.

The measurement of TR using proportional chambers is generally based on one or both of two methods:

- the “charge measurement” method, where the signal collected from a chamber wire is amplified with a time constant of a few hundred ns and then charge analyzed by ADCs [22];
- the “cluster counting” method, where the wire signal is sharply differentiated in order to discriminate the δ -ray background from the clusters of ionization from X-ray photoelectrons producing pulses (hits) exceeding a threshold amplitude [23].

In each case a cut on the analyzed charge or on the number of clusters discriminates radiating particles from slower nonradiating ones.

1.2 Detector description

We have built three TRD modules, each of about 12 m^2 surface area for the MACRO experiment [24, 25] at the Gran Sasso Laboratory (LNGS). The laboratory is located at an average depth of 3700 hg/cm^2 , with a minimum depth of 3200 hg/cm^2 . The differential distribution of the residual energy of the downgoing muons is expected to be nearly flat up to 100 GeV, falling rapidly in the TeV region. The mean muon energy is a few hundred GeV [26]. The TRD was designed to explore the muon energy range from 100 GeV to 1 TeV. Below this energy range there is no TR emission for the radiator parameters chosen. In the range 0.1–1 TeV the response versus γ is approximately linear. For energies greater than 1 TeV, where the muon flux is estimated to be a few percent of the total, the TR response is saturated.

In order to study the energy spectrum of multimMuon events, a large area TRD with relatively fine spatial resolution is required. The total multiple muon event rate for MACRO is roughly 0.015 Hz, and the average separation of muons within an event is of the order of a few meters

[27]. In order to obtain a reasonable sample of these events a detector with an area of several tens of square meters is needed.

For the TRD active detector we have adopted 6 meter long proportional counters having a $6 \times 6 \text{ cm}^2$ square cross section. The polystyrene walls of the counters are slightly thinner than 1 mm. The proportional tube cross section of $6 \times 6 \text{ cm}^2$ is a compromise between efficiently converting the TR photons in an argon-based gas mixture, while at the same time maintaining the ionization energy loss of the muon at a relatively low level. The design parameters were checked by calculations based on a Monte Carlo [29] and from tests in a pion/electron beam at energies 1–5 GeV, covering the Lorentz factor interval $10^3 < \gamma < 10^4$ [28].

A layer of these counters is placed between each radiator layer, forming a large multiple layer TRD. The TRD units were installed on the floor of the upper MACRO detector with the proportional counters running parallel to the streamer tubes, simplifying the track reconstruction. The number of TRD layers was fixed at ten in order to constrain the number of channels, and to take into account the 2 meter maximum available height for a detector inside MACRO. The radiator thickness was limited for the same reason to 10 cm. Each TRD module has an active volume of $6 \times 1.92 \times 1.7 \text{ m}^3$ and contains 32 tubes per layer, interleaved with the foam radiators. The bottom tube layer is placed on an eleventh radiator. In this way, the detector is symmetric with respect to downgoing and upgoing muons, thus offering the additional opportunity for measuring the energy of neutrino induced upgoing muons.

The radiator material used was Ethafoam 220, having a density of 35 g/l, and cells of approximately 0.9 mm diameter and $35 \mu\text{m}$ wall thickness [30]. These cell dimensions provide a relatively wide range between γ_{th} and γ_{sat} . The TR spectra from Ethafoam of equivalent density have already been measured by many authors [7, 30, 31] and match properly with the transmission characteristics of the proportional tube wall.

A reduced scale prototype exposed to a pion/electron test beam was used to determine the response function of the detector, and to develop and test the TRD readout electronics. In two recent papers [21, 28] we have analyzed the behavior of the TR energy versus γ by the method of charge analyzing the signal, and, in addition, we have investigated the dependence of the number of TR photons versus γ . We found that the dependence on γ of the number of photons is quite similar to that of the TR energy, as has been previously reported by other authors [32]. Therefore, we have equipped the TRD with cluster counting electronics, since this method has proven to be more reliable and less expensive than the “charge measurement” method.

The total cluster count (total number of hits) measured in the TRD follows a Poisson distribution with an average number of hits of the order of ten. In Fig. 1 we show the average number of hits for Ethafoam at various γ and beam crossing angles. The average number of hits obtained from electrons without radiators is indicated for normal incidence. The response curves show a behavior compatible with the relativistic rise ($\gamma < 100$) and the Fermi plateau for the energy loss of a fast particle.

In Fig. 2 we show a computer display of a multi-muon event in the MACRO/TRD detector. The muons enter MACRO from the top, pass through the TRD, and then exit through the lower MACRO detector. The TRD readout trigger is provided by the MACRO muon trigger [25]. In this display the number of hits produced by the muons are indicated by different symbols.

2 Data selection

In this analysis we consider the data collected from April 1995 to August 1997 by the first TRD module. A selection was made to disregard those MACRO runs in which the TRD was affected

by stability problems or was malfunctioning. We started with a raw data sample of 4665 runs, in which 215184 muons entered the TRD. This initial sample consisted of 185915 single muons, 19875 double muons and 9394 muons in events of high multiplicity. Since the TRD calibration was performed with particles crossing all ten detector layers and at zenith angles below 45° [28], in the present analysis only single muons meeting these constraints have been included. Runs having muon rates more than three standard deviations with respect to the average have been excluded.

To evaluate the muon energy, we sum the number of TRD hits along the straight line fit to the track reconstructed by the MACRO streamer tubes (Fig. 2). The distribution of deviations between the reconstructed track and TRD hits is Gaussian, with a standard deviation of $\sigma=1.86$ cm. In reconstructing a track, we consider only the tubes within 3σ of the track.

In order to understand the effects of long term detector gain variations, we have calculated the average number of hits for single muons collected in each run. The distribution is Gaussian, with an average number of hits equal to 4.31 and a standard deviation $\sigma=1.0$. Those runs with averages fell outside three standard deviations from the mean have been excluded. The excluded runs suffered from gas gain drifts or from occasional power failures. The final data sample consists of 60256 single muons, for a livetime of about 560.5 days. The reduction of this sample to roughly 1/3 of the raw data sample is mainly due to the requirement that the muons cross ten TRD planes.

3 Muon energy spectrum

In Fig. 3 the distribution of the number of hits in the single muon tracks in the final event sample is shown. The slope change which occurs at roughly $n_{hits} = 15$ is due to the TRD response saturation at an energy of about 1 TeV. This distribution is then used to obtain the single muon energy spectrum.

We have used an unfolding technique, following the prescriptions of refs.[33, 34]. Unfolding methods require that the distribution must be limited to a finite interval. When this condition is not fulfilled, as for the cosmic ray energy spectrum, the method cannot be automatically applied. However, in our case the detector response is flat outside the 0.1–1 TeV energy interval, thus ensuring that the measured quantity, namely the number of hits, becomes effectively “bounded”.

3.1 Detector response

The distribution of the hits collected along a muon track by the TRD at a given zenith and azimuth angle, $N(k, \theta, \phi)$, can be related to the residual energy distribution of muons, $N(E, \theta, \phi)$, by

$$N(k, \theta, \phi) = \sum_j p(k | E_j, \theta, \phi) N(E_j, \theta, \phi) \quad (1)$$

where the detector response function, $p(k | E_j, \theta, \phi)$, is the probability to observe k hits in a track of a given energy E_j and at a given angle θ and ϕ . This response function must contain both the detector acceptance and the event reconstruction efficiency. We derived this function by simulating MACRO using GEANT [35], including the simulation of trigger efficiency. The TRD simulation was based on the test beam calibration data [28] (Fig. 1).

As shown in Fig. 1, the TRD exhibits a different behavior in different energy regions. It provides a flat response below 100 GeV, a linear increasing response up to about 1 TeV, and then saturates. The energy bins used in presenting the muon energy spectrum were chosen on

the basis of this behavior, and on the basis of the momentum bins used in the calibration runs. The first bin covers the energy range from 0 to 50 GeV, while the last represents a lower limit at 1 TeV corresponding approximately to the TRD saturation energy for muons. On the same basis we have chosen four angular bins from 0 to 45 degrees.

The detector response function was derived using an unbiased muon energy spectrum, i.e., one which was flat versus energy, θ and ϕ . It was calculated by taking the ratio of the number of events producing k hits at a given energy and incident angle θ to the total number of the events in the same energy bin and incident angle. The simulated data were produced in a form similar to experimental data, in order to process it with the same analysis procedure.

Low energy muon data was used to verify the consistency of the simulation with the behavior of the TRD during data taking. We selected muons with $\gamma < 20$ (corresponding to an average energy of about 1.5 GeV) which cross the TRD and then stop in the lower MACRO detector, and muons with large scattering angles in the lower part of MACRO. The selection of muons stopping in the MACRO layers below the TRD was based on considering only tracks crossing less than eight out of ten layers of the lower MACRO structure.

The average number of hits versus zenith angle is shown in Fig. 4 together with the same average hit distribution simulated by Monte Carlo procedure described above. The experimental data are in good agreement both with the Monte Carlo and with the TRD calibration points of the equivalent energy, namely for $\gamma < 20$ (Fig. 1).

3.2 Results

The unfolding procedure described above was applied to the TRD experimental data, starting with a trial spectrum assigned to the unfolded distribution [33, 34] according to a local energy spectrum of muons at 4000 hg/cm² with a spectral index of 3.7 as reported in [36]:

$$N_0(E, \theta, \phi) \sim e^{-\beta h(\alpha-1)}(E + \epsilon(1 - e^{-\beta h}))^{-\alpha}. \quad (2)$$

The parameters are: $h = 4$ km w.e., $\alpha = 3.7$, $\beta = 0.383$ (km w.e.)⁻¹ and $\epsilon = 0.618$ TeV.

The iterative procedure of the unfolding method is terminated when the reconstructed distribution at the i th iteration is equivalent to the previous one at a probability $\geq 99\%$. The χ^2 is calculated by summing over the squared differences between the channel content of two subsequent distributions, normalized to the square of the statistical errors. The final result is found to be unaffected by the choice of the spectral index in the initial probability function.

In Figs. 5 and 6 the muon energy differential spectrum and the muon energy integral spectrum are reported. Fig. 7 shows the average energy of events below 1 TeV versus rock depth, while Fig. 8 shows the fraction of muons with energies exceeding 1 TeV versus rock depth. The fraction is about 6%, independent of rock depth. A topographic map of the terrain above MACRO was used to obtain the rock depth from the direction of the muon track. The average muon energy in the energy range $0.1 < E < 1$ TeV is 225 ± 3 (stat.) ± 4 (syst.) GeV. The quoted systematic errors are due to beam calibration uncertainties, estimated at $\pm 2\%$. They have been obtained by changing the calibration input data in the unfolding procedure by the same percentage. The statistical and systematic errors have been added in quadrature in the figures.

The single muon spectrum deep underground is determined by the spectrum at the surface and by the energy losses in the rock. In this analysis we have investigated the consistency of the residual muon energy spectrum with the “all-nucleon” energy spectrum of primary cosmic rays. We have compared our measurements to the predictions from two extreme hypotheses

on the primary spectra [37] assuming a given range of the spectral index, namely the “Light” (i.e., proton-rich) [38] and the “Heavy” (i.e., Fe-rich) [39] compositions. In the present analysis we have adopted a normalization procedure for these compositions in order to reproduce the known abundances and spectra directly measured, and to match the extensive air shower data at higher energies [27]. The interaction of the cosmic rays in the atmosphere was simulated with the HEMAS code [40]. The secondary muons at sea level were propagated through the rock, with the muon energy loss in the rock evaluated according to the prescriptions of ref. [36]. The rock thickness was calculated at each θ and ϕ from the Gran Sasso map [5]. We used the correction procedure described in ref. [41] for the conversion to standard rock. We find that our measurements of the average single muon energy and the fraction of single muons with energy ≥ 1 TeV are in agreement with spectra obtained from the Monte Carlo models.

The experimental average muon energy over all energies was calculated by adding to the average energy obtained with an energy cut at 1 TeV the contribution from muons of greater energy. The high energy contribution was estimated by multiplying the measured fraction of muons with energy ≥ 1 TeV by the average muon energy above 1 TeV:

$$\langle E_\mu \rangle = (1 - f) \cdot \langle E_\mu \rangle_{cut} + f \cdot \langle E_\mu \rangle_{nocut} \quad (3)$$

where f is the fraction of events with $E \geq 1$ TeV (measured), $\langle E \rangle_{cut}$ is the average energy with $E < 1$ TeV (measured) and $\langle E \rangle_{nocut}$ is the average energy with $E \geq 1$ TeV.

The evaluation of $\langle E \rangle_{nocut}$ was based on a simple extrapolation of the local energy spectrum as reported in Eqn. (2) using the same parameters $\alpha = 3.7$, $\beta = 0.383 \text{ (km w.e.)}^{-1}$ and $\epsilon = 0.618$ TeV for the depth interval shown in Figs. 7 and 8. The average muon energy obtained in this way is $320 \pm 4(\text{stat.}) \pm 11(\text{syst.})$ GeV and does not change appreciably with variation of these parameters. A variation of 3% in the above parameters, as is typically quoted by various authors (e.g., ref. [42]), implies uncertainties of about 0.1% for β , 0.2% for ϵ and 1% for α . These uncertainties are significantly less than our quoted error.

Fig. 9 shows the average single muon energy as a function of rock depth. Also shown are the predictions of the two composition models studied. The NUSEX experimental point is also shown, and is in good agreement with our measurements. The present result is not able to discriminate between the two composition models.

4 Conclusions

We have measured directly the residual energy of cosmic ray muons at the Gran Sasso underground laboratory, using a TRD which has been operational since April 1994. The average single muon energy, in the range 0.1–1 TeV, is 225 ± 3 (stat.) ± 4 (syst.) GeV. The fraction of muons with energies > 1 TeV is 6.0 ± 0.1 (stat.) ± 0.4 (syst.)% in the depth range 3150–6500 hg/cm². Treating the events with energies greater than 1 TeV in the manner described above, the average single muon energy in this depth range is 320 ± 4 (stat.) ± 11 (syst.) GeV. The results are in agreement with the calculations of the energy loss of the muons in the rock above the detector.

References

- [1] M. Calicchio et al., Phys. Lett. **B 193** (1987) 131

- [2] M. Castellano et al., Nucl. Instr. and Meth. **A 256** (1987) 38
- [3] C. Castagnoli et al., Phys. Rev **D 52** (1995) 2673
- [4] C. Castagnoli et al., Astr. Phys. **6** (1997) 187
- [5] The MACRO Collaboration (M. Ambrosio et al.), Phys. Rev. **D 52** (1995) 3793
- [6] B. Dolgoshein, Nucl. Instr. and Meth. **A 326** (1993) 434
- [7] T. A. Prince et al., Nucl. Instr. and Meth. **123** (1975) 231
- [8] G. Hartman et al., Phys. Rev. Lett. **38** (1977) 368
- [9] S. P. Swordy et al., Nucl. Instr. and Meth. **193** (1982) 591
- [10] K. K. Tang, The Astroph. Journ. **278** (1984) 881
- [11] J. L’Heureux, Nucl. Instr. and Meth. **A 295** (1990) 245
- [12] R. L. Golden et al., The Astr. Journ. **457** (1996) L103
- [13] E. Barbarito et al. Nucl. Instr. and Meth. **A 357** (1995) 588
- [14] M. L. Cherry, Workshop on High Energy Cosmic Ray Interactions, Salt Lake City (1983)
- [15] K. G. Antonian et al., XXIII Conference on Cosmic Ray Physics, H.E.7.1 (1987)
- [16] V. L. Ginzburg and I. M. Frank, JETP **16** (1946) 15
- [17] G. M. Garibian, Sov. Phys. JETP **6** (1958) 1079
- [18] J. Cobb et al., Nucl. Instr. and Meth. **140** (1977) 413
- [19] X. Artru et al., Phys. Rev. **D 12** (1975) 1289
- [20] A. Bungener et al., Nucl. Instr. and Meth. **214** (1983) 261
- [21] R. Bellotti et al., Nucl. Instr. and Meth. **A 305** (1991) 192
- [22] J. Fischer et al., Nucl. Instr. and Meth. **127** (1975) 525
- [23] C. W. Fabjan et al., Nucl. Instr. and Meth. **185** (1981) 119
- [24] The MACRO Collaboration (C. De Marzo et al.), Nuovo Cimento **9 C** (1986) 281
- [25] The MACRO Collaboration (S. P. Ahlen et al.), Nucl. Instr. and Meth. **A 324** (1993) 337
- [26] L. Bergamasco et al., Nuovo Cimento C6 (1983) 569
- [27] The MACRO Collaboration (S. P. Ahlen et al.), Phys. Rev. **D 46** (1992) 4836
- [28] E. Barbarito et al. Nucl. Instr. and Meth. **A 365** (1995) 214; The MACRO Collaboration (M. Ambrosio et al.), Proc. XXIV ICRC, Rome, **1** (1995) 1031
- [29] M. Castellano et al., Comput. Phys. Commun. **61** (1990) 395

- [30] C.W. Fabjan, Nucl. Instr. and Meth., **146** (1977) 343
- [31] M. L. Cherry, Phys. Rev. **D 17** (1978) 2245
- [32] A. Denissov et al., Preprint Fermilab Conf. 84/134E (1984)
- [33] G. D'Agostini, Nucl. Instr. and Meth., **A 362** (1995) 487
- [34] M.N. Mazziotta, **LNGS 52/95**, July 1995
- [35] R. Brun et al., CERN Publication DD/EE/84-1 (1992)
- [36] P. Lipari and T. Stanev, Phys. Rev. **D 44** (1991), 3543
- [37] The MACRO Collaboration (M. Ambrosio et al.), Phys. Rev. **D 56** (1997) 1418
- [38] C. Fichtel and J. Linsley, Astrophys. J. **300** (1986) 474
- [39] J. A. Goodman et al., Phys. Rev. Lett. **42**, (1979) 854; J. A. Goodman et al., Phys. Rev. **D 26**, (1982) 1043
- [40] C. Forti et al., Phys. Rev. **D 42** (1990) 3668
- [41] A. G. Wright, Proc. of 12th ICRC, Denver (USA), **3** (1973) 1709
- [42] G. Battistoni et al., Nucl. Instr. and Meth., **A 394** (1997) 136

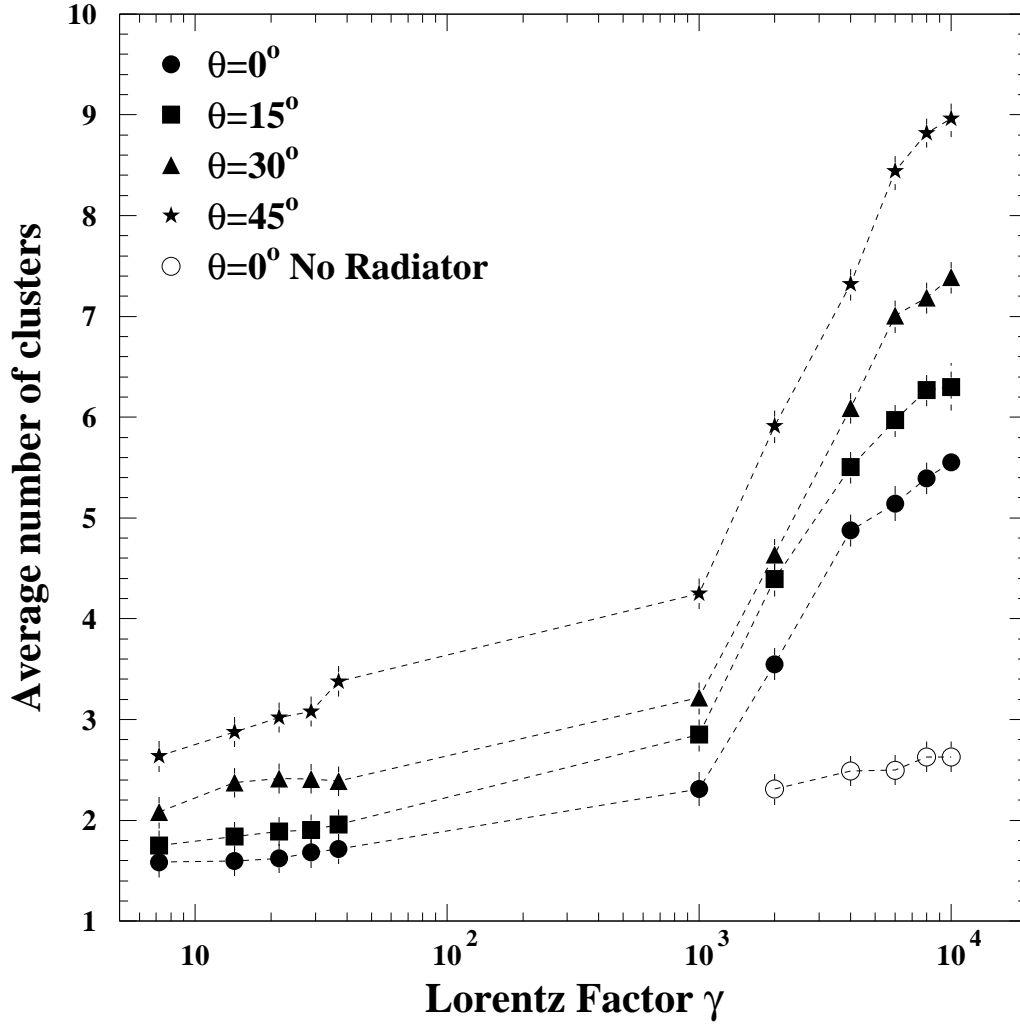


Figure 1: Average number of hits plotted versus the Lorentz factor γ for several beam crossing angles. Dots: 0° incident beam angle; open circles: 0° beam angle without radiator; squares: 15° beam angle; triangles: 30° beam angle; stars: 45° beam angle. The dashed lines are drawn to guide the eye.

MACRO

RUN 10959 EVENT 10334 at 18:34:48.0 on 22/9/95

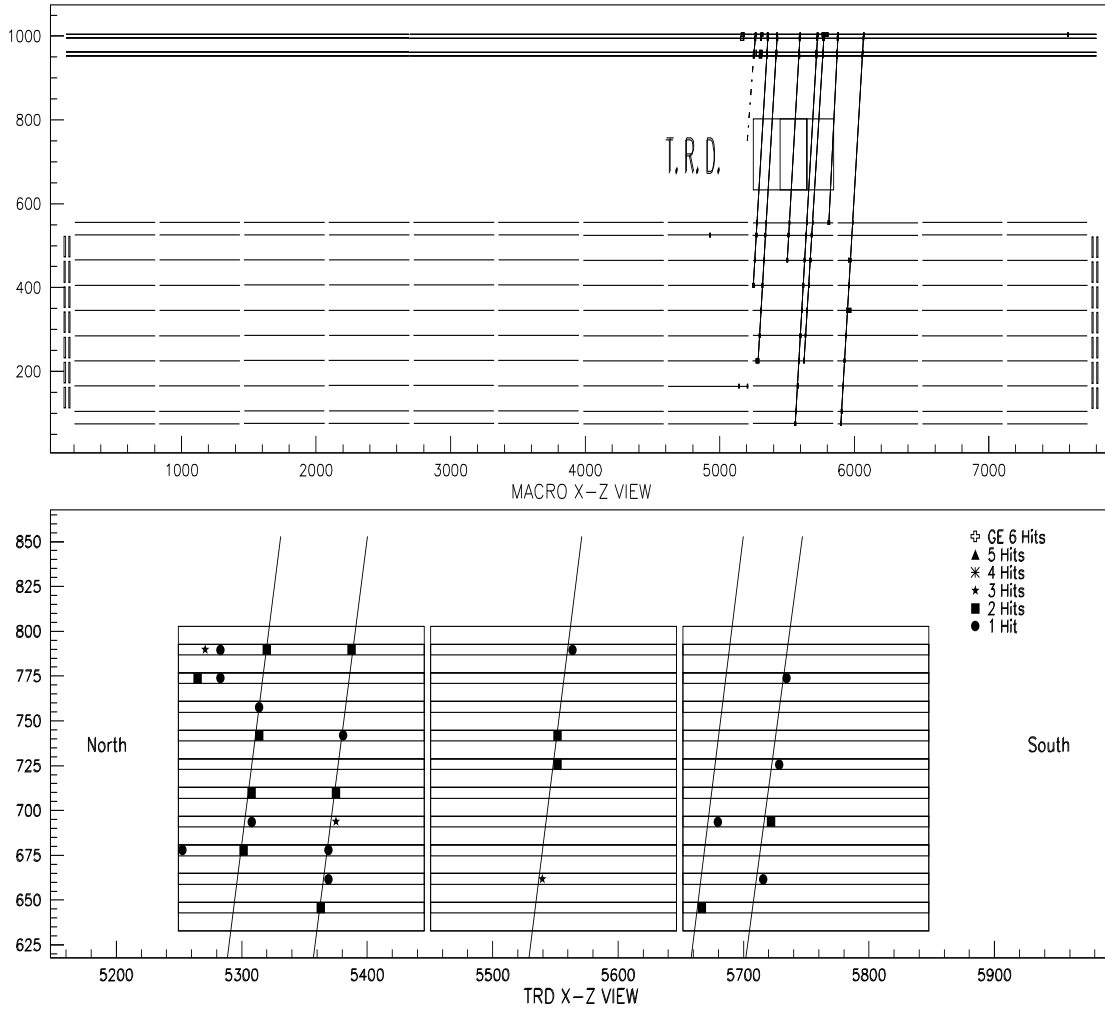


Figure 2: Display of a multiple muon event crossing MACRO and the TRD. The upper part of figure shows the whole MACRO detector in the view orthogonal to the streamer tubes, while in the lower part only the TRD in the view orthogonal to proportional tubes is shown. The number of hits produced in the TRD are shown by different symbols. While the second muon from the right has E_μ approximately 200 GeV, the other muons have energies of roughly 500 GeV.

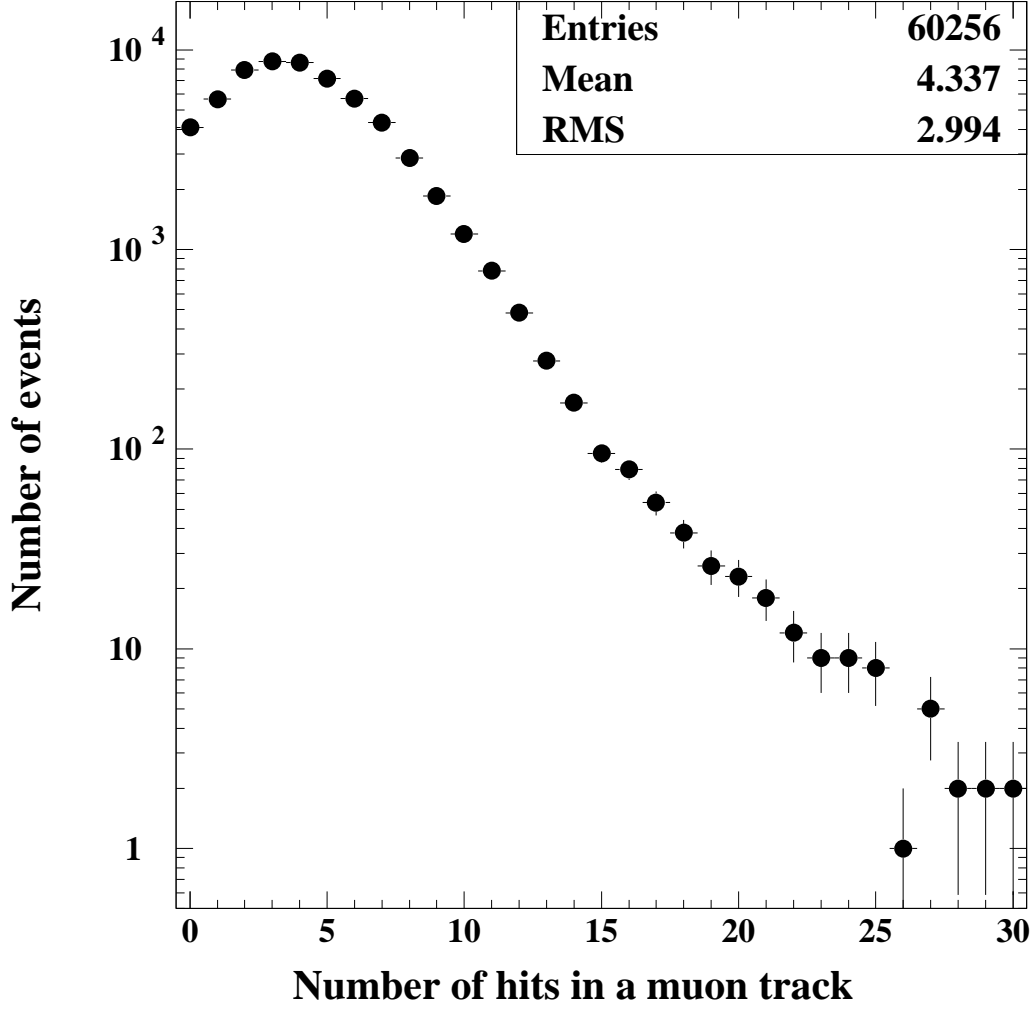


Figure 3: Hit distribution for single muon tracks crossing the 10 TRD planes with zenith angles less than 45° . Only statistical errors are shown.

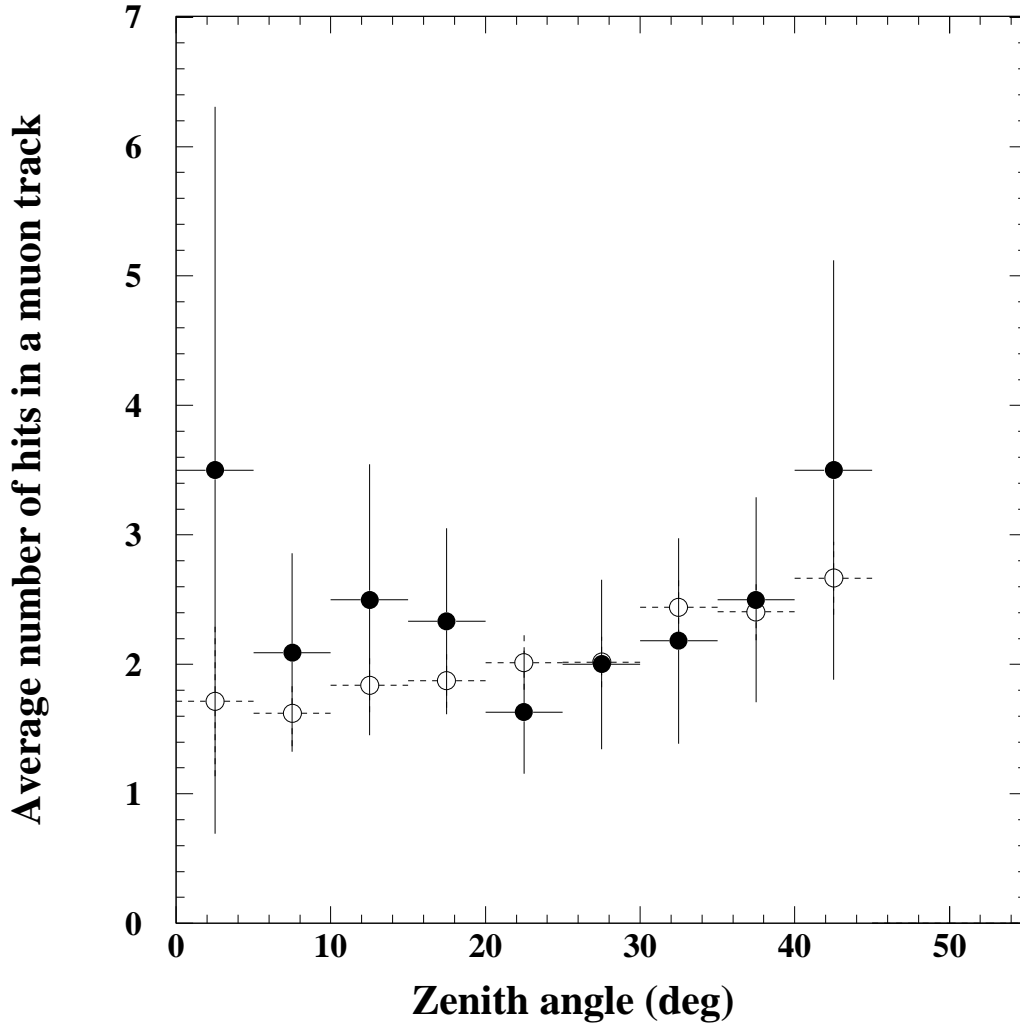


Figure 4: Average number of hits versus zenith angle for muons crossing the TRD and stopping in the lower MACRO detector. Black circles: TRD data; open circles: Monte Carlo simulation. Only statistical errors are shown.

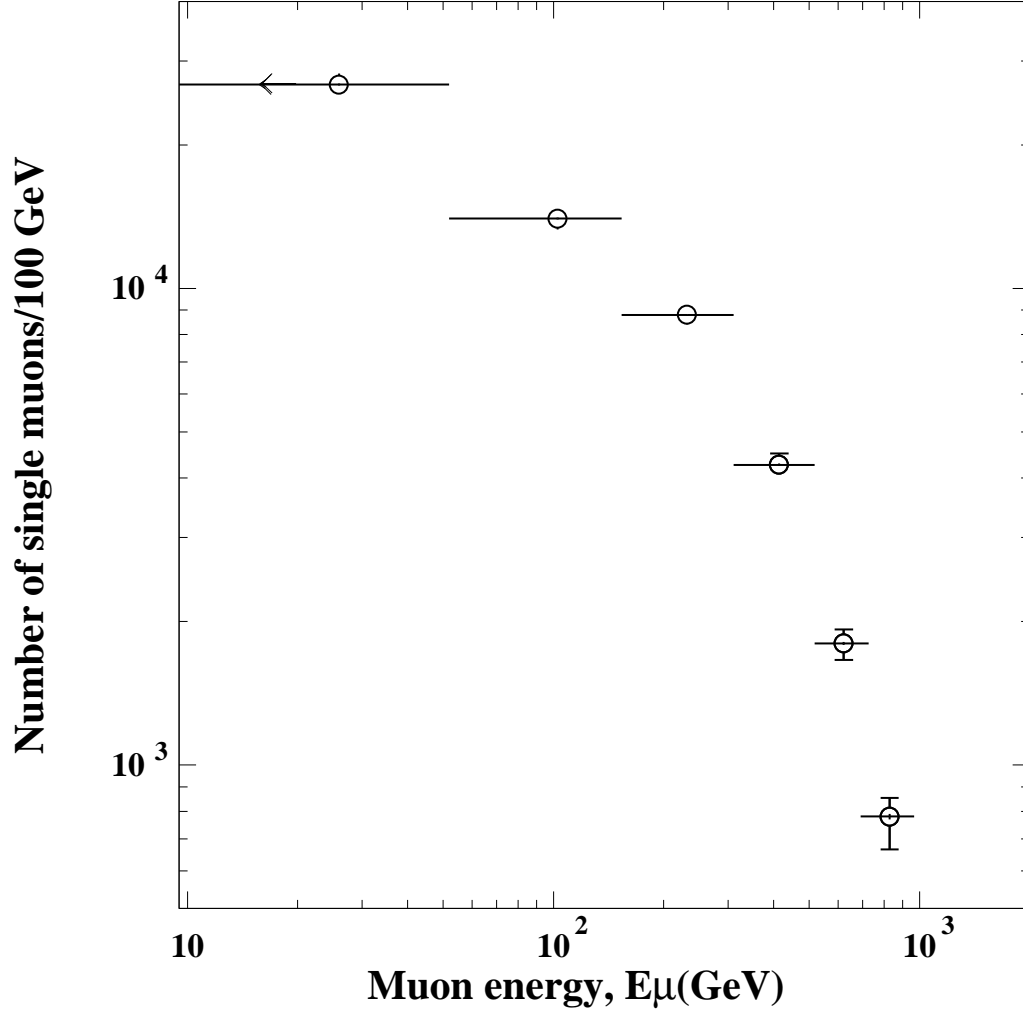


Figure 5: Differential energy distribution of single muons with zenith angle $\leq 45^\circ$ measured with the TRD. The spectrum was obtained by unfolding the hit distribution shown in Fig. 3.

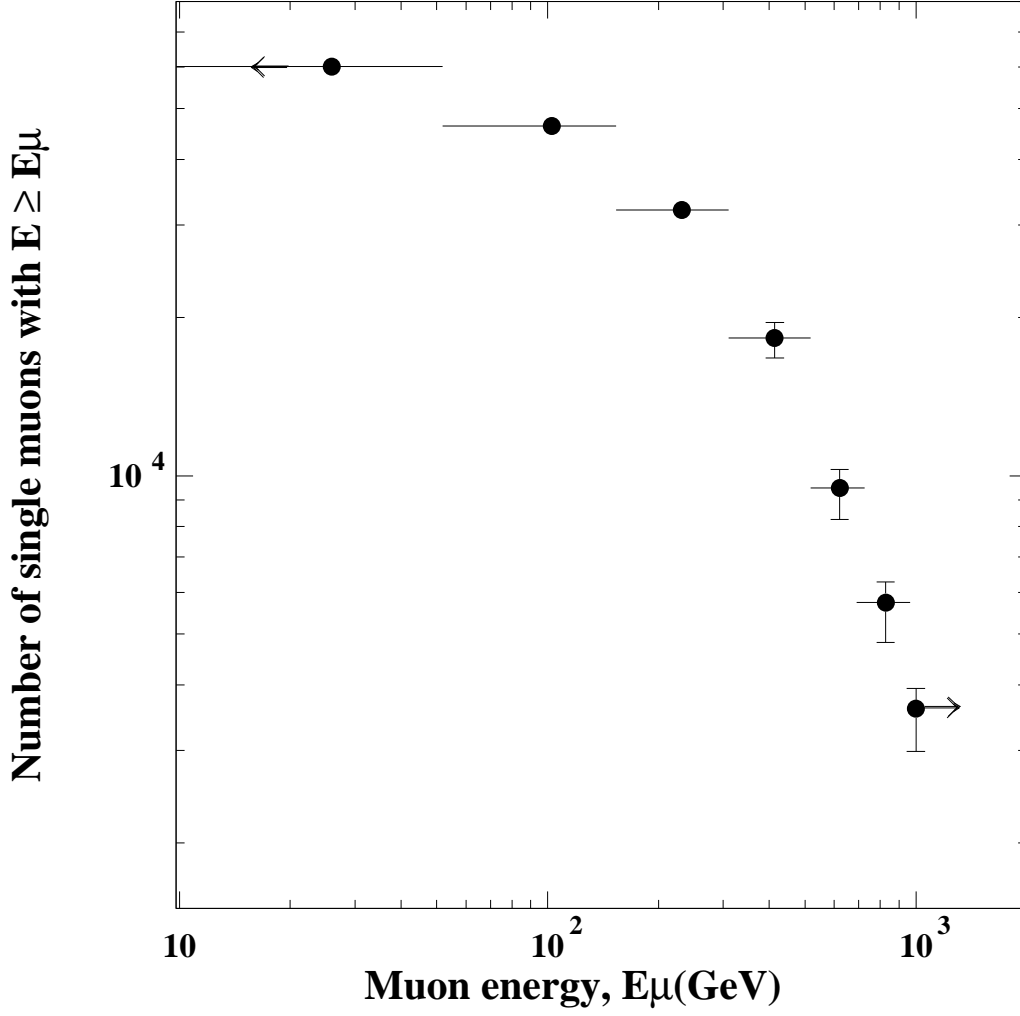


Figure 6: Integral energy distribution of single muons with zenith angle $\leq 45^\circ$ measured with the TRD. The spectrum was obtained by unfolding the hit distribution shown in Fig. 3.

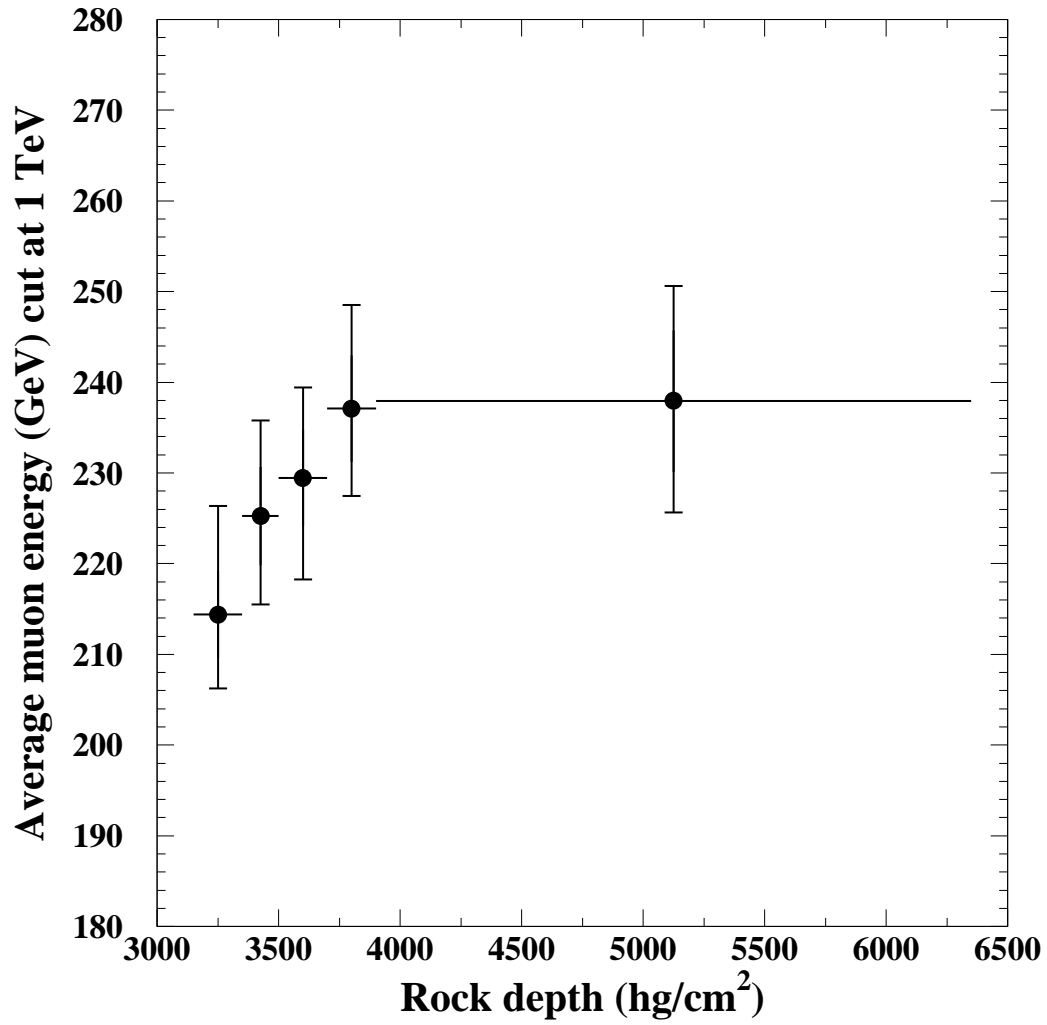


Figure 7: Average single muon energy, computed with a cut at 1 TeV, versus the standard rock depth.

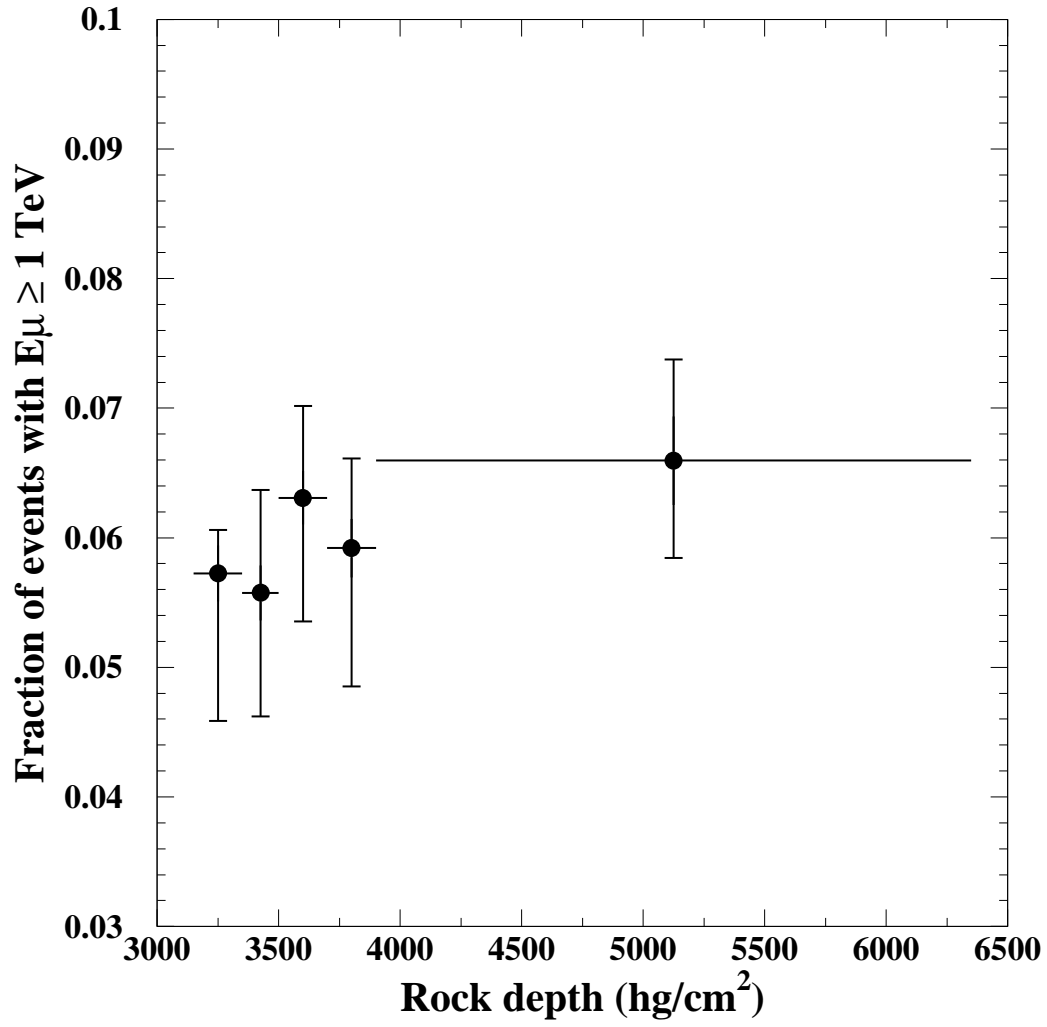


Figure 8: Fraction of single muons with energy greater than 1 TeV versus the standard rock depth.

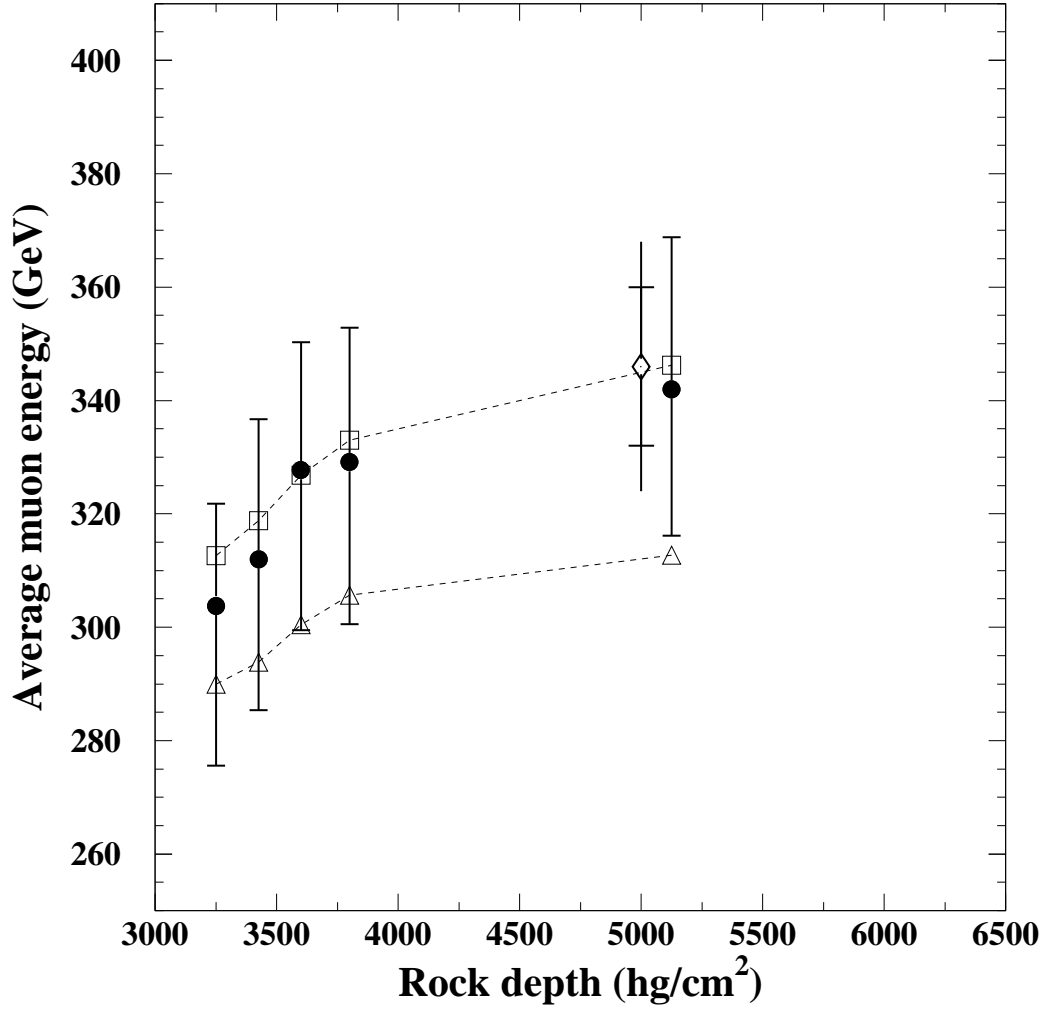


Figure 9: Average single muon energy measured by the MACRO TRD (black circles) versus standard rock depth. The open symbols connected by dashed lines are the predictions of a HEMAS-based Monte Carlo for the “Light” (squares) and “Heavy” (triangles) composition models. The result reported by the NUSEX experiment is shown by the diamond (the extensions of the error bar represents the systematic uncertainty added in quadrature to the statistical error [4]).